Metallurgy and Foundry Engineering – Vol. 41, 2015, No. 4, pp. 171–180
http://dx.doi.org/10.7494/mafe.2015.41.4.171

Janusz Krawczyk, Piotr Bała, Łukasz Frocisz, Tomasz Tokarski, Bogdan Pawłowski

The influence of microstructure of 30MnB4 steel on hydrogen-assisted cracking

Wpływ mikrostruktury stali 30MnB4 na pękanie wodorowe

Abstract
This paper analyzes the problem of susceptibility to hydrogen-assisted cracking (fracture behavior) of zinc-coated screws made of 30MnB4 steel. Two samples (screws) were compared after proper and improper heat treatment affecting hydrogen solubility during the further galvanic process and resulting in different fracture modes. Both samples were loaded to failure by torsion. The fracture surface and microstructure of the samples were examined using scanning electron microscopy (SEM) and energy dispersive X-ray spectroscopy (EDS).

Keywords: hydrogen-assisted cracking, hydrogen trapping, zinc coating, toughened steel

Streszczenie
Praca dotyczy problemu pękania wspomaganego wodorem. Materiałem do badań były śruby ocynkowane wykonane ze stali 30MnB4. Porównywano dwie próbki po poprawnej obróbce cieplnej, obejmującej hartowanie i niskie odpuszczanie, oraz obróbce polegającej wyłącznie na hartowaniu. Sposób przeprowadzenia obróbki cieplnej skutkował zmianami w rozpuszczalności wodoru w strukturze analizowanej stali. Wodór dostarczony został do materiału podczas procesu elektrolitycznego pokrywania cynkiem. Po procesie cynkowania obie próbki były skręcane do zerwania. Powstałe przełomy i zgłady metalograficzne badanych materiałów obserwowano przy wykorzystaniu skaningowego mikroskopu elektronowego (SEM), dokonano również analizy ich składu chemicznego, wykorzystując metodę spektroskopii rentgenowskiej z dyspersją energii fali (EDS).

Słowa kluczowe: pękanie wspomagane wodorem, pułapkowanie wodoru, cynkowanie, stal ulepszona cieplnie

1. Introduction

Due to its high anti-corrosive properties, electrolytic zinc coating is one of the easiest ways to prevent rust on screws. However, during the galvanic process, atomic hydrogen

Janusz Krawczyk Ph.D. D.Sc. Eng., Bogdan Pawłowski Ph.D. D.Sc. Eng., Łukasz Frocisz M.Sc. Eng.: AGH University of Science and Technology, Faculty of Metals Engineering and Industrial Computer Science, Krakow, Poland; **Piotr Bała Ph.D. D.Sc. Eng.:** AGH University of Science and Technology, Faculty of Metals Engineering and Industrial Computer Science, Krakow, Poland, Academic Centre for Materials and Nanotechnology, Krakow, Poland; **Tomasz Tokarski Ph.D. Eng.:** AGH University of Science and Technology, Faculty of Non-Ferrous Metals, Krakow, Poland; jkrawcz@agh.edu.pl

can be absorbed into the steel microstructure, which can result in hydrogen embrittlement (sometimes called internal hydrogen assisted cracking [1–3]). The higher the tensile strength of the steel, the greater the risk of its cracking. It has been found [4–7] that susceptibility to hydrogen-assisted cracking in toughened steels is mainly connected with the effect of tempering on the solubility of hydrogen in the steel microstructure (hydrogen trapping).

This paper analyzes the fracture behavior of zinc-coated screws made of 30MnB4 steel after proper and improper heat treatment followed by baking performed as a means of dehydrogenation.

2. Examined procedure and material

The material used in this study was a commercial low-alloy 30MnB4 steel, widely used for screw fabrication. Quenched and tempered (tempering at 410°C) screws made of this steel were electrolytically zinc-coated with an Fe/Zn12c1B layer followed by baking at 200°C for 5 h. The microstructure of the investigated screw after this process (no. 1) is shown in Figures 1 and 2. For the purpose of this work, zinc coating was performed for the quenched screw but not the tempered.

The microstructure of the screw after this process (no. 2) is shown in Figures 3–5. The morphology of the carbides in the screw after Process no. 1, its distribution, and quantity responds to the microstructure expected after quenching and tempering at 410°C (Fig. 2). The higher number of smaller carbides observed in the microstructure of the screw after Process no. 2 as compared to the screw after Process no. 1 responds to the microstructure expected after quenching and low tempering (Fig. 3).

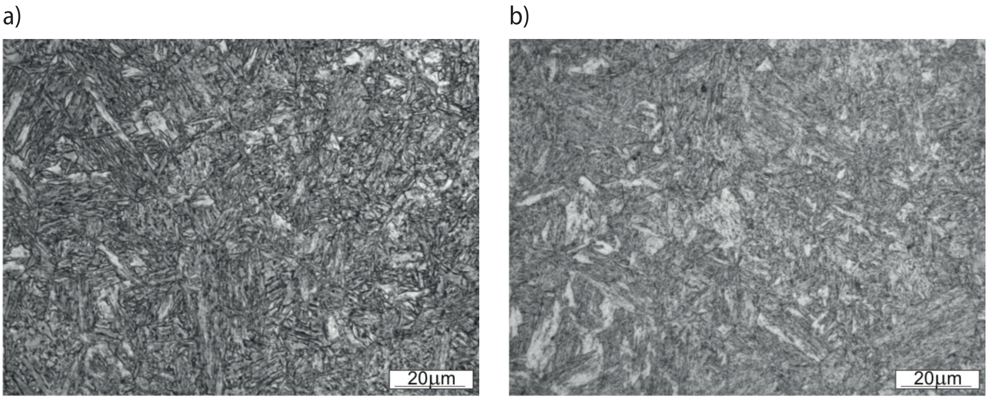

Fig. 1. Cross-sectional microstructure of screws after Process no. 1, light microscope: a) screw no. 1; b) screw no. 2; etched with 2% nital

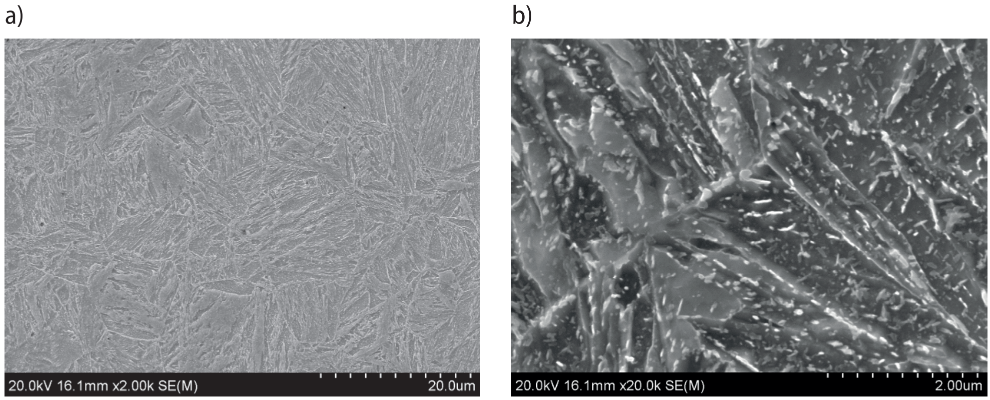

Fig. 2. Cross-sectional microstructure of screw after Process no. 1 (screw no. 1), SEM; etched with 2% nital magn. x2000 (a) and x20000 (b)

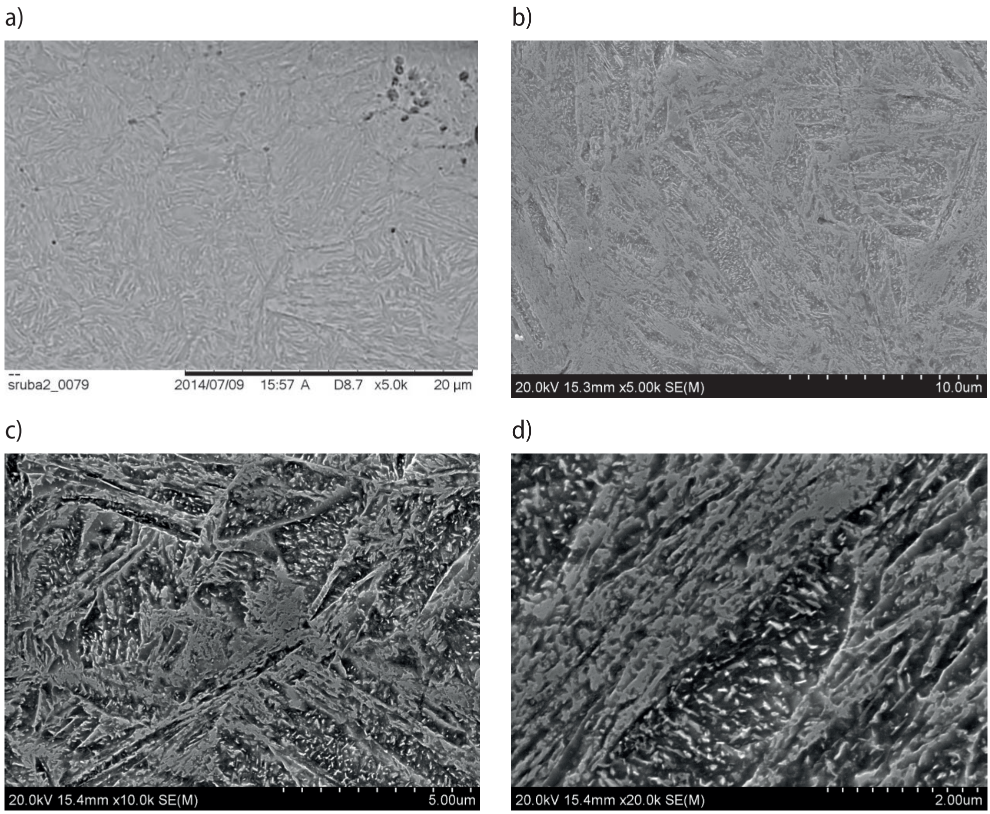

Fig. 3. Cross-sectional microstructure of screw after Process no. 2: a) subsurface below zinc layer; (b–d) area in core of screw; SEM; etched with 2% nital

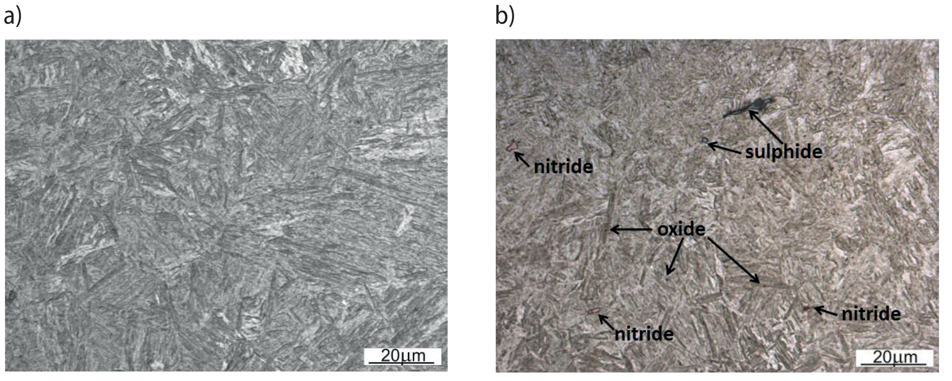

Fig. 4. Cross-sectional microstructure of screw after Process no. 2, light microscope: a) microstructure; b) non-metallic inclusions morphology; etched with 2% nital

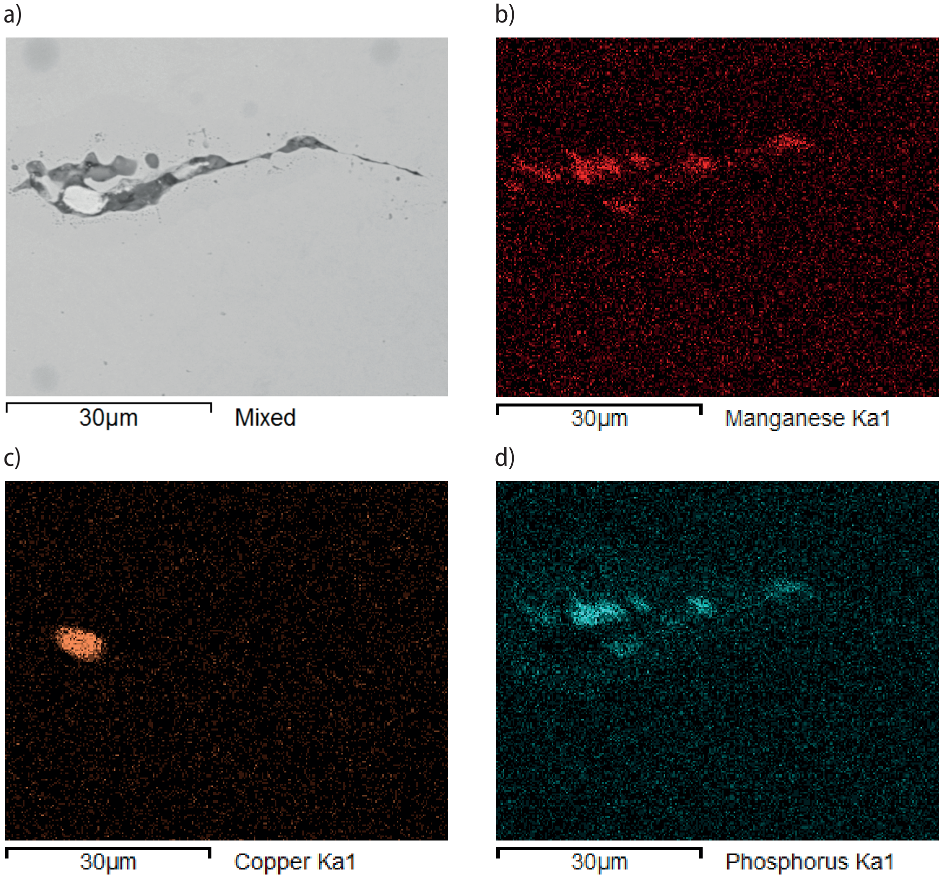

Fig. 5. EDS element map from conglomerate of non-metallic inclusions and copper in cross-section of screw after Process no. 2: area in core of screw: a) SEM; (b–d) EDS element map

3. Results and discussion

For the screw after Process no. 1, the zinc coating is uniform and proper (Fig. 6). In the case of the screw processed according to Treatment no. 2, the zinc layer is not uniform; however, numerous examples of zinc diffusion in the areas of the subsurface cracks are shown (Fig. 7).

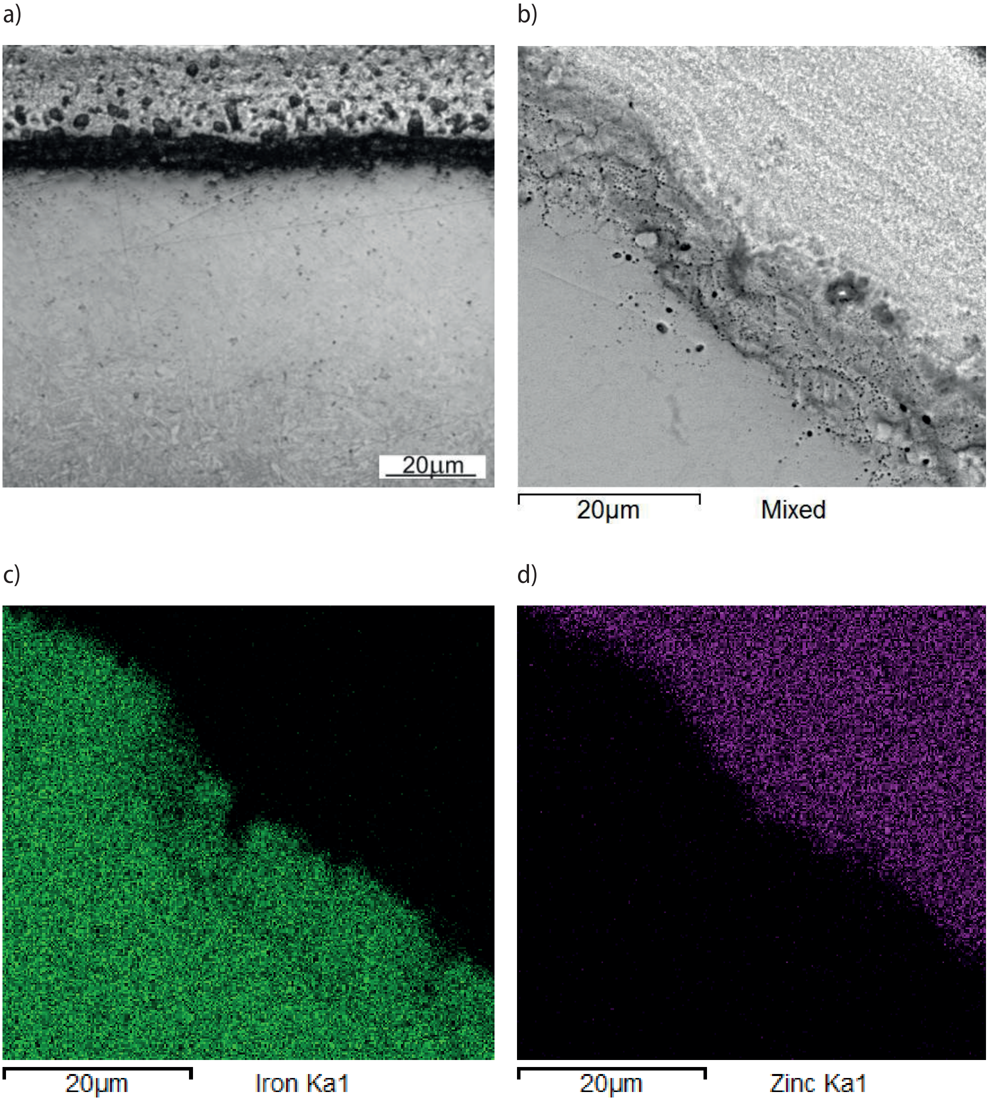

Fig. 6. Zinc coating of screw after Process no. 1: a) light microscopy; b) SEM; (c, d) EDS element map

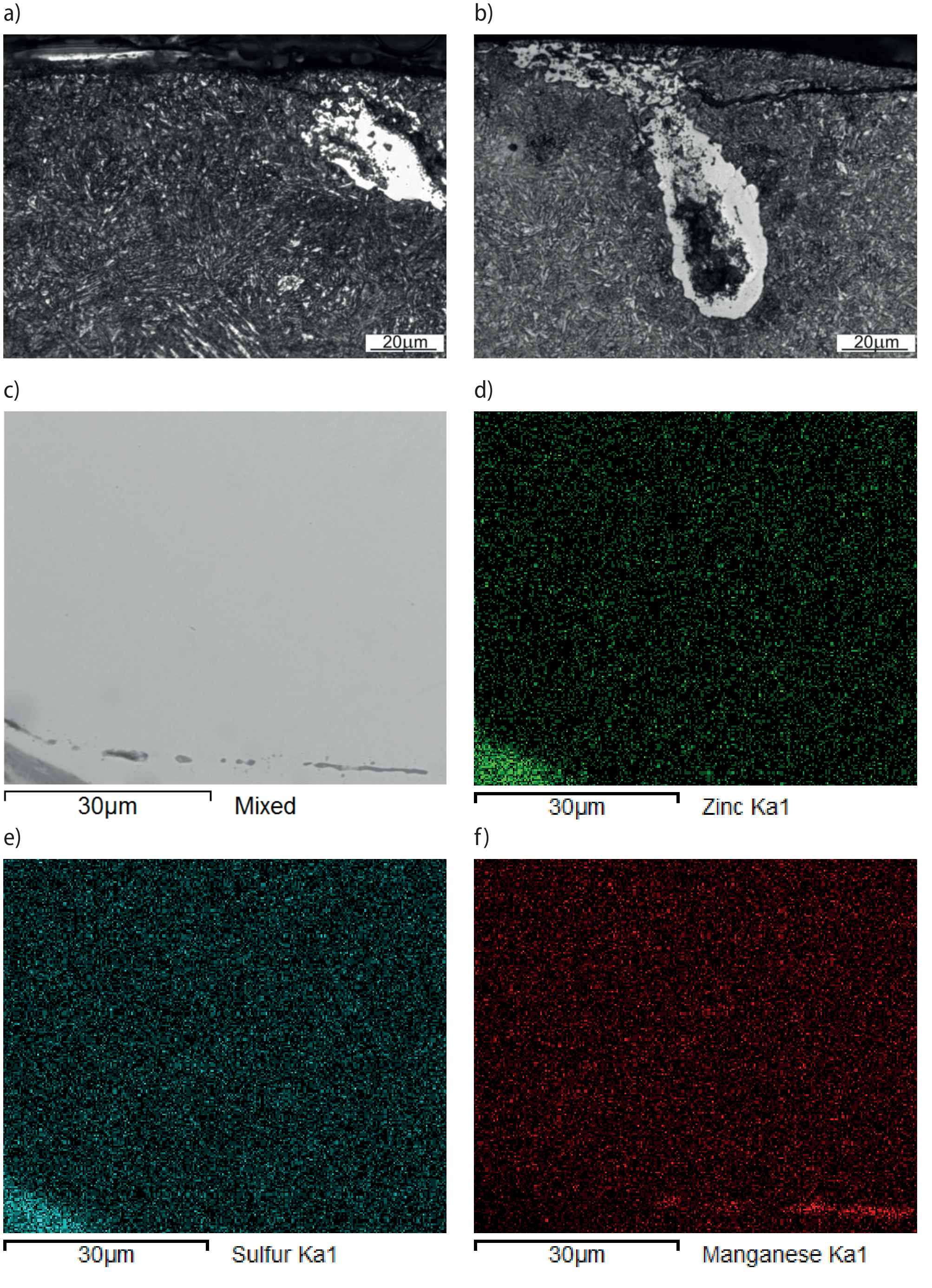

Fig. 7. Zinc coating of screw after Process no. 2: (a, b) light microscopy; c) SEM; (d–f) EDS element map

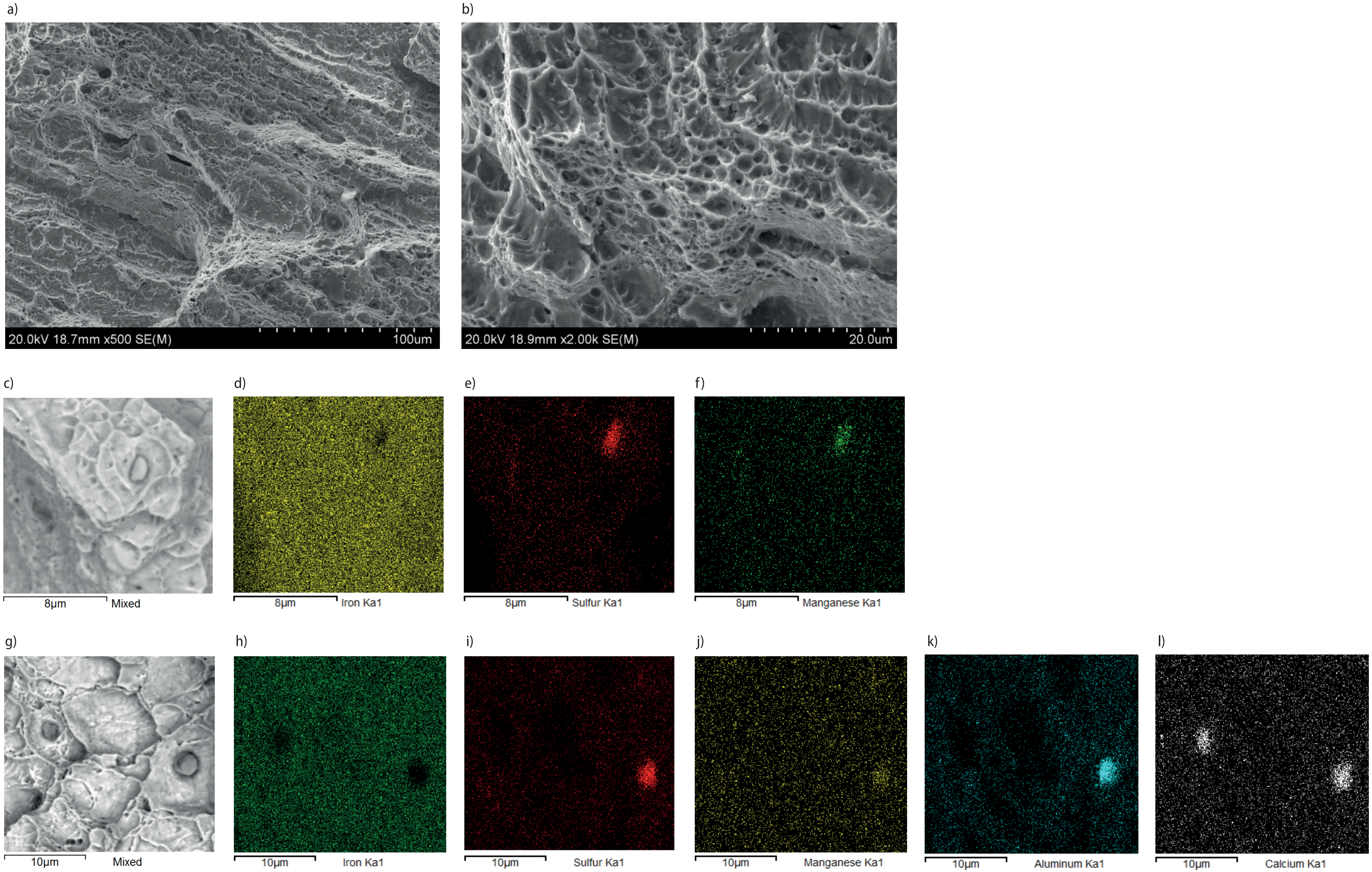

Fig. 8. Fracture of screw after Process no. 1, ruptured under laboratory conditions: a–b) SEM; c) surface for EDS analysis; d–f) EDS element map of area from Figure 8c; g) surface for EDS analysis; h–l) EDS element maps of area from Figure 8g

For the screw after Process no. 1, hardness values were within a range of 360–373 HV. For the screw after Process no. 2, hardness was higher (450–459 HV).

The higher number of carbides in the sample after Process no. 2 favors hydrogen trapping. Hydrogen accumulated in the stress area around the precipitations.

The rupture surface of the screw after Process no. 1 has only a transcrystalline, ductile, dimpled character (Fig. 8; on the interleaf).

The rupture surface of the screw after Process no. 2 has two distinctly different areas (Fig. 9). In the area further from the surface, it shows a transcrystalline ductile fracture, a so-called dimpled rupture (Fig. 10). In the area closer to the surface, it shows a brittle intergranular fracture, indicating the occurrence of decohesion at the grain boundaries (Fig. 11).

This brittle intergranular fracture corresponds to the hydrogen-assisted cracking [8, 9]. The process that exposes the steel to hydrogenation is galvanization [10, 11]. The effect of hydrogen on the mechanical behavior of steels is twofold: it affects its local yield strength, and it accelerates material damage. On the other hand, the diffusion behavior is influenced by hydrostatic stress, plastic deformation, and the strain rate. This requires hydrogen sorption and diffusion [12–16]. For this reason, trapping and diffusion of the hydrogen depends on the microstructure [17].

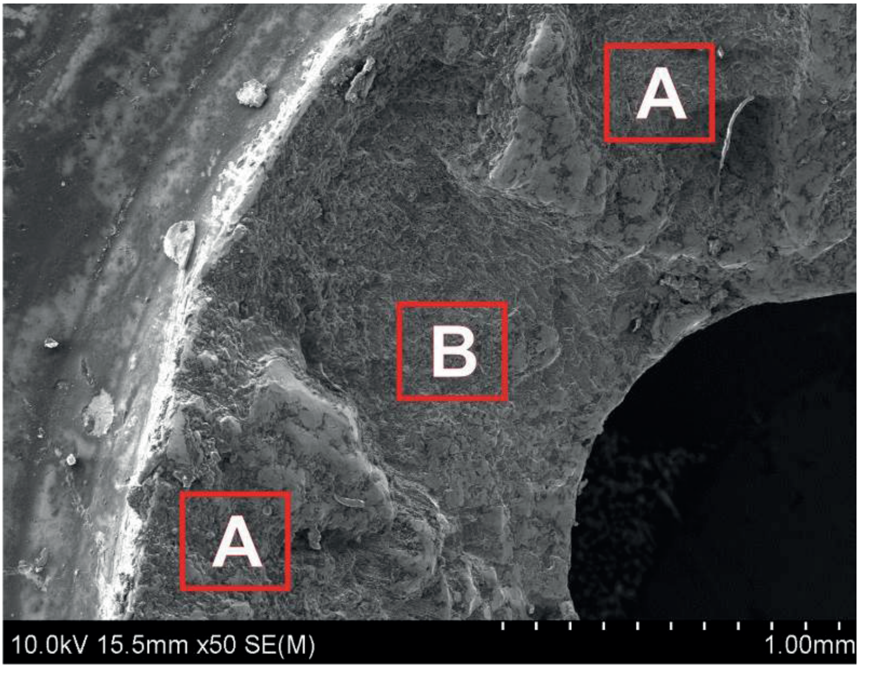

Fig. 9. Fractography of screw after Process no. 2 with two distinctly different areas (A and B)

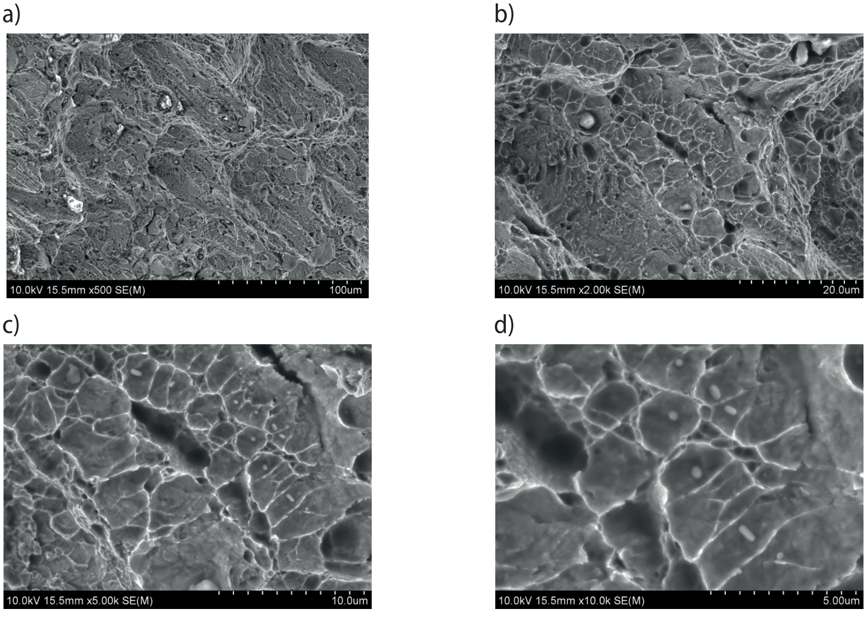

Fig. 10. Fracture surface of Area A further from screw surface, screw after Process no. 2, SEM, magn. ×500 (a); ×2000 (b); ×5000 (c) and ×10000 (d)

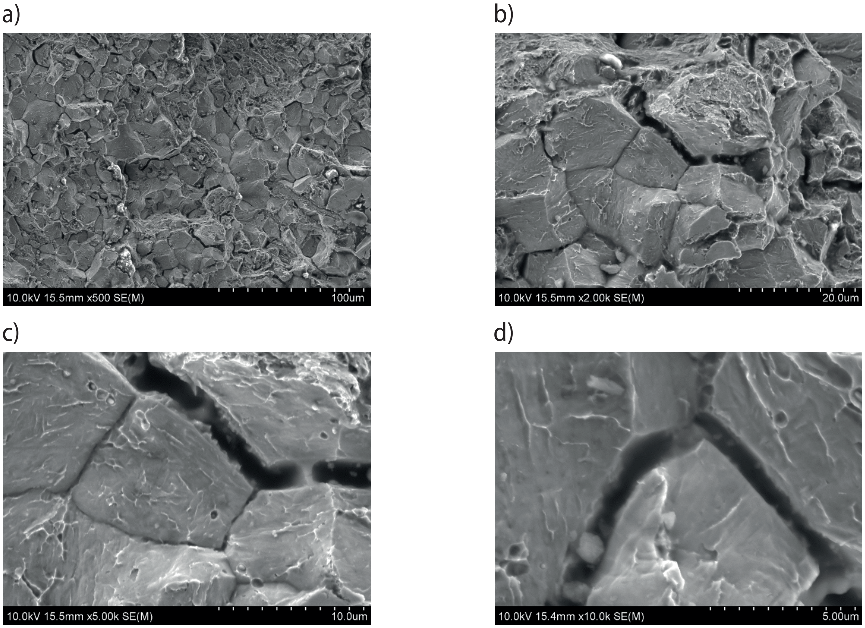

Fig. 11. Fracture surface of Area B further away from screw surface, screw after Process no. 2, SEM, magn. ×500 (a); ×2000 (b); ×5000 (c) and ×10000 (d)

4. Conclusions

The results presented in this work allow us to formulate the following conclusions:

1. The microstructure of the sample (screw) quenched but not tempered (Process no. 2) has a high number of carbides as compared to the sample (screw) quenched and tempered (Process no. 1). Carbides precipitated during baking at 200°C were visible on SEM images in the screw after Process no. 2,
2. The rupture surface of the screw after Process no. 2 has two distinctly different areas. In the area further from the surface of the screw, it shows a transcrystalline ductile fracture, a so-called dimpled rupture. In the area closer to the surface, it shows a brittle intergranular fracture, indicating the occurrence of decohesion at the grain boundaries. In the screw after Process no. 1, the entire rupture area shows a transcrystalline ductile fracture.
3. Most likely, the brittle intergranular fracture is caused by the presence of hydrogen in the microstructure of the screw after Process no. 2 (coming from the electrolytically zinc coating).
4. The density of defects in martensite and lower bainite favors the trapping of hydrogen. The tempered sample has a lower density of defects. The trapping of hydrogen at the carbide/matrix interfacial boundaries required a greater amount of time to absorb the amount of hydrogen required for the initiation of hydrogen assisted-cracking.

References

[1] Gangloff R.P.: Critical Issues in Hydrogen Assisted Cracking of Structural Alloys. In: Shipilov S. (ed.): Environment Induced Cracking of Metals. Elsevier Science, UK, Oxford 2006

[2] Stahle R.W., Hochmann J., McCright R.D., Slater J.E. (eds.): Stress Corrosion Cracking and Hydrogen Embrittlement of Iron Base Alloys. NACE, Houston, TX, 1977

[3] Hydrogen in Metals. Procedings of the 2nd International Congress, Pergamon Press, Paris, France, 6–10 June 1977

[4] Pawlowski B.: Effect of microstructure on stress corrosion cracking of Cr-Mn-Si-Ni steel. Materials and Corrosion, 37, 8 (1986), 448–451

[5] Mazur A., Pawlowski B.: The stress corrosion cracking of high strength Cr-Mn-Si-Ni and Cr-Mo steels. Corrosion Science, 26, 1 (1986), 7–14

[6] Pawlowski B., Mazur A. , Gorczyca S. : The effect of the tempering processes on the susceptibility to stress corrosion cracking of high strength steel. Corrosion Science, 32, 7 (1991), 685–691

[7] Sanoğlu F.: The effect of tempering on susceptibility to stress corrosion cracking of AISi 4140 steel in 33% sodium hydroxide at 80°C. Materials Science and Engineering A, 315, 1–2 (2001), 98–102

[8] Gangloff R.P., Somerday B.P. (eds.): Gaseous hydrogen embrittlement of hydrogen in energy technologies, Vol. 2. Mechanism, modelling and future developments. Woodhead Publishing, UK, Cambridge (2012)

[9] Demouchy S.: Hydrogen diffusion in spinel grain boundaries and consequences for chemical homogenization in hydrous peridotite. Contributions to Mineralogy and Petrology, 160, 6 (2010), 887–898

[10] Urednicek M., Kirkaldy J.S.: Mechanism of iron attack inhibition arising from additions of aluminum to liquid Zn(Fe) during galvanizing. Zeitschrift für Metallkunde, 64 (1987), 649

[11] Okafor I.C., O'Malley R.J., Prayakarao K.R., Aglan H.A.: Effect of zinc galvanization on the microstructure and Fracture Behavior of Low and Medium Carbon Structural Steels. Engineering, 5, 8 (2013), 656–666

[12] Sieverts A. : The absorption of Gases by Metals. Zeitschrift für Metallkunde, 21 (1929), 37–46

[13] Dadfarnia M., Sofronis P., Somerday B.P., Robertson I.M.: On the small scale character of the stress and hydrogen concentration fields at the tip of an axial crack in steel pipeline: effect of hydrogen-induced softening on void growth. International Journal of Materials Research, 99, 5 (2008), 557–570

[14] Falkenberg R., Brocks W., Dietzel W., Scheider I.: Modelling the effect of hydrogen on ductile tearing resistance of steels.International Journal of Materials Research, 101, 8 (2010), 989–996

[15] Ramachandran E.G., Ruge J.: The effect of hydrogen on the hardness of steel. Zeitschrift für Metallkunde 80, 5 (1989), 359–360

[16] Wu X.Q., Kim I.S.: Influence of charged hydrogen on tensile behavior of a pressure vessel steel at relatively high temperatures. Zeitschrift für Metallkunde 94, 9 (2003), 1017–1020

[17] Timmins P.F.: Solutions to Hydrogen attack in steels. Materials Park, OH, ASM International, 1997